Nucl. Sci. and Tech., Vol.13, No. 1 (2023), pp. 01-09

Nuclear Science and Technology

Journal homepage: http://jnst.vn/index.php/nst

Development of Brain MRI Image Segmentation program using UNET++ network for radiosurgery planning

B. N. Ha[1], N. T. Kien[1], T. T. Duong[1], T. N. Toan[2], H. Q. Tuan[2], P.C.Phuong[3], P.V. Thai[3], V. T. Trang[4]

[1] *Hanoi University of Science and Technology*
[2] *Vietnam Atomic Energy Institute*
[3] *Nuclear Medicine and Oncology Center at Bach Mai Hospital*
[4] *Thuongmai University*
Email: ha.buingoc@hust.edu.vn

Abstract: Image processing is one of the most important and widely used techniques in the medical field. Magnetic Resonance Imaging (MRI) can provide diagnostic images with high contrast and high resolution, especially for low-density tissue. Therefore, applications to support tumor prediction are researched and developed. In this paper, we applied artificial intelligence to identify and detect tumors and use the UNET++ deep learning model, which achieved results with a recognition rate of about 80%. The results for a great deal of built-in functionality in the built-in physician support software system in practice.

Keywords: *Image processing, magnetic resonance imaging (MRI), UNET++, deep learning model, artificial intelligence, neurons.*

I. INTRODUCTION

Magnetic Resonance Imaging (MRI) is a diagnostic imaging technique commonly used in medical imaging. MRI research has been conducted since the 1940s, and the first clinical MRI images were taken in the 1980s. MRI images show a higher contrast of soft tissue than CT images. Therefore, MRI is especially useful in diagnosing issues involving the nervous system, such as the brain, spine, and knee joints [1]. Clinical MRI imaging is commonly used to explore brain structure, evaluate brain lesions, and identify neurological disorders such as Alzheimer's disease and multiple sclerosis [2, 3]. In addition, MRI images are also commonly used to conduct radiosurgery planning in treating brain cancer [4].

Image segmentation is an essential task in imaging diagnosis and disease treatment. The purpose of segmentation is to group pixels with the same properties into a group, from which agencies and organizations present in the diagnostic image can be segregated separately. Through image segmentation, radiologists can detect abnormalities and lesions for diagnosis, treatment planning as well as evaluation of treatment results [5]. Image segmentation is a complex task, and the quality of the segmentation process is highly dependent on the image quality, image type, and complex structure of the captured image. The segmentation of magnetic resonance images is a complicated task. Factors that influence the precision of the segmentation process are the electronic noise of image acquisition, the bias field (characterized by smooth changes in intensity within tissue), and the partial volume effect due to the intensity of a voxel contributed by various tissue types.

https://doi.org/10.53747/nst.v13i1.398
Received 29 November 2022, accepted 03 October 2023

Image segmentation is divided into three main methods: manual segmentation, semi-automatic segmentation, and automatic segmentation. Manual segmentation is performed entirely by experienced radiologists. The manual segmentation process is highly time-consuming and has many subjective errors because of radiologist fatigue in the diagnostic process. With the development of computer science and technology, automatic and semi-automatic segmentation methods have been deployed to assist doctors in shortening the diagnosis time and reducing errors in the diagnosis process.

Semi-automatic and automatic segmentation tasks are divided into two main methods: classical computer vision approaches and artificial intelligence (AI) - based techniques. Numerous research groups have implemented image segmentation using the classical computer vision method for a long time. The typical techniques commonly used are the automatic thresholding method, edge detection method, edge capture method, statistical segmentation, and regional growth segmentation method [6-10]. In recent years, with the development of data science and artificial intelligence, computers have been increasingly used in medical imaging [11]. Research groups apply many machine-learning techniques to classify and segment MRI images. Traditional machine learning techniques often have low performance with big datasets and complex structured images [12], which makes it difficult to detect anomalies and perform automatic segmentation accurately. The limitations of traditional machine learning methods can be improved using deep learning methods. Deep learning methods can be used for quantitative analysis of MRI images through self-learning of features contained in the images. With the rapid development of CNN networks, deep learning shows potential in the automatic analysis of medical images [13, 14]. The modern CNN model is increasingly improved to give it the ability to segment images with high accuracy [15, 16].

There is currently no standard MRI dataset in Vietnam to train deep learning models. Due to domestic MRI imaging equipment's characteristics, most brain MRIs used in hospitals are T1 images. At the same time, the training dataset available worldwide includes other types of MRI images, such as T2 and FLAIR. Therefore, it is impossible to directly use models trained with international datasets for segmentation of MRI images at domestic hospitals. Therefore, this research aims to build an automated brain tumor segmentation program from magnetic resonance imaging using the UNET++ deep learning model [16]. The trained model is capable of segmenting MRI images collected at hospitals in Vietnam; the model can assist doctors in the treatment planning of brain cancer radiosurgery.

II. SUBJECTS AND METHODS

A. Data

The training dataset used in this study is the data in the BraTS2020 dataset [17-19] combined with the MRI data collected at Bach Mai Hospital. The BraTS2020 dataset contains brain MRI slices of 369 patients; each patient's data includes four image types: native (T1), post-contrast T1-weighted (T1Gd), T2-weighted (T2) and T2 Fluid Attenuated Inversion Recovery (T2-FLAIR). The dataset is manually segmented by one to four experienced radiologists. The tumors of patients in the dataset were classified and annotated into three groups: enhancing tumors (ET), peritumoral edematous tissue (ED), and core necrotic tumor

- necrotic tumor core (NRC). MRI data from Bach Mai Hospital includes DICOM files containing brain MRI slices. Most MRI images used for radiosurgery planning at Bach Mai are T1 images containing markers and the skull in each slice. Since the data in radiotherapy planning is only T1 images, we only took T1 images from the BraTS2020 and Bach Mai's datasets to combine into the training dataset for this study. To homogenize the images from the BraTS2020 and Bach Mai's datasets, we performed image processing to remove the marker and skull present in the image.

The training dataset is also processed to reduce overfitting using a technique called data augmentation. Data augmentation techniques used include Biased crop (random cropping of data with probability 0.4), Flips (flip the image along X and Y axes with probability 0.5), Gaussian Noise (add Gaussian noise with mean zero and standard deviation uniformly sampled in the range [0, 0.33] with probability 0.15), Gaussian Blur (add Gaussian blurring with mean zero and standard deviation uniformly sampled in the range [0.5, 1.5] with probability 0.15) and Brightness (brightness is adjusted randomly between 0.7 and 1.3 with probability 0.15).

The dataset we obtained from Bach Mai Hospital consists of 100 T1 images from 100 distinct patients. The BraTS2020BachMai dataset utilized in this study is T1 imaging data from 469 different patients after homogenization with the BraTS2020 and other data processing. For district training, we used data from 251 patients, 59 patients for the test set, and 159 patients for the validation set (val).

B. Model

UNET++ has been proven to be more efficient and achieves significantly more excellent performance than UNET by redesigning lines that eliminate the connection between the encoder and decoder sub-networks [16]. Figure 1 depicts the structure of the UNET++ network; compared to the UNET network, UNET++ adds up-sampling blocks at each down-sampling layer on the encoder sub-network (backbone), forming a dense convolutional block instead of just having skip pathways between the encoder and the decoder sub-network as in UNET. A concatenation layer is placed before each convolution block in the dense convolution to fuse the output of the previous convolutional layer with the corresponding up-sampling output of the lower dense block. The redesign of the skip connection paths makes the semantic level of the feature map on the encoder and decoder more proportional. Therefore, the optimizer can quickly identify whether the feature map from the encoder and decoder is semantically similar or not. We can calculate the output xi, j of node Xi, j where i is the index of the down-sampling layer and j is the index of the convolutional layer, as follows [16]:

$$x^{i,j} = \begin{cases} \mathrm{H}\left(x^{i-1,j}\right) & \mathrm{j} = 0 \\ \mathrm{H}\left(\left[\left[x^{i,k}\right]_{k=0}^{j-1}, U\left(x^{i+1,j-1}\right)\right]\right) & \mathrm{j} > 0 \end{cases} \quad (1)$$

Where H(.) is the convolution operator associated with the activation function, U(.) is the up-sampling operator, and [] stands for the association class. From Figure 1, we can see that nodes with j = 0 receive only one input from the previous layer on the encoder, nodes with j = 1 have two inputs, both inputs are from the encoder, and nodes with j > 1 have j +1 input, where j input is the output of previous nodes on the same connection skipping path, and one input is the result of up-sampling the lower layer on the encoder.

The workflow for the brain MRI image segmentation program is shown in Figure 2.

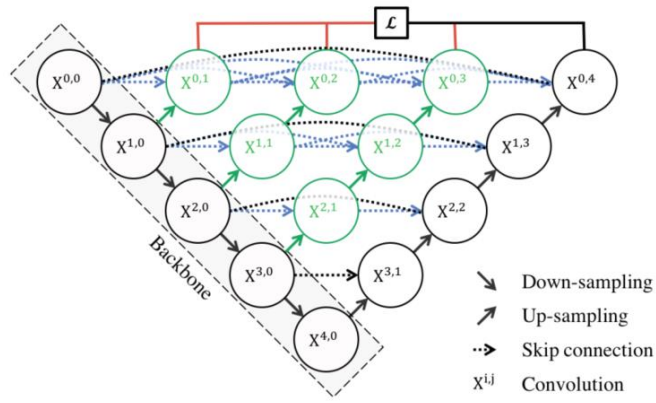

Fig. 1. The architecture of UNET++ [16]

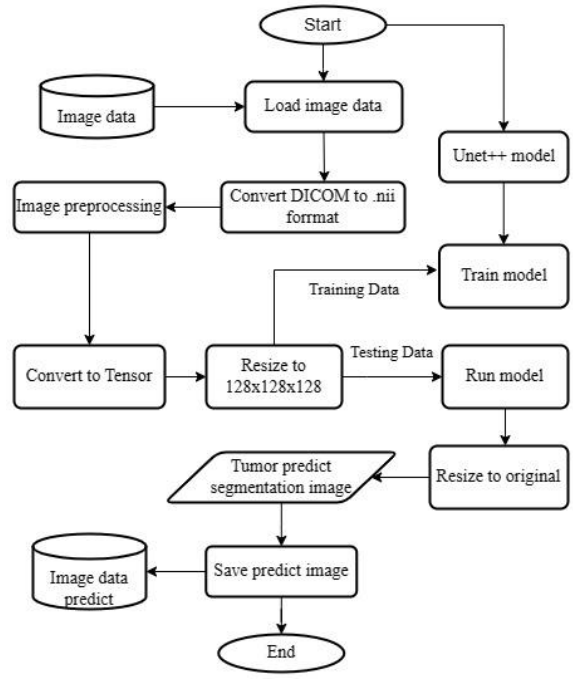

Fig. 2. The workflow for the brain MRI image segmentation program

C. Performance Metrics

During the training process, the model always tries to change its internal parameters to recognize and analyze the input data. The weight change process is done based on the gradient descent algorithm. The loss function is a valuable tool to evaluate the learning ability of the model with the suitable weights. The loss function is essential in making the learning process more efficient when an appropriate weight is found. For UNET++ networks, the Focal Tversky Loss function has been shown to perform best when segmenting lesions [17]. The Focal Tversky Loss function of the object labeled x is described in the following formula [17].

$$\mathrm{FTL}_x = \sum_x \left(1 - \frac{\sum_{i=1}^{N} p_{ix} g_{ix} + \varepsilon}{\sum_{i=1}^{N} p_{ix} g_{ix} + \alpha \sum_{i=1}^{N} p_{i\tilde{x}} g_{ix} + \beta \sum_{i=1}^{N} p_{ix} g_{i\tilde{x}} + \varepsilon}\right)^{1/\gamma} \quad (2)$$

In this paper, we use two evaluation tools, namely the Dice Coefficient and the IoU

(Intersection over Union) coefficient, to evaluate the performance and accuracy of the trained model. The dice coefficient is used to evaluate the similarity of two samples widely used in image processing recognition and is expressed as a formula [18].

$$\mathrm{DSC} = \frac{2TP}{2TP + FP + FN} = \frac{2|X \cap Y|}{|X| + |Y|} \quad (3)$$

The IoU coefficient is a coefficient that quantifies the degree of overlap between the prediction result and the diagnostic result, expressed in the form of the formula [18].

$$IoU = \frac{|X \cap Y|}{|X \cup Y|} \quad (4)$$

Where |X| and |Y| are the tumor segmented by model and the ground truth segmented by physician, respectively. TP, FP, and FN are true positives (TP), false positives (FP), and false negatives (FN), respectively.

III. RESULTS AND DISCUSSION

A. Results

Figures 3 and 4 show the results of preprocessing the training data. The MRI data collected from Bach Mai Hospital had the skull removed to create similarities with the data in the BraTS2020 dataset (Figure 3). After the skull stripping, the entire data will be augmented with the results shown in Figure 4.

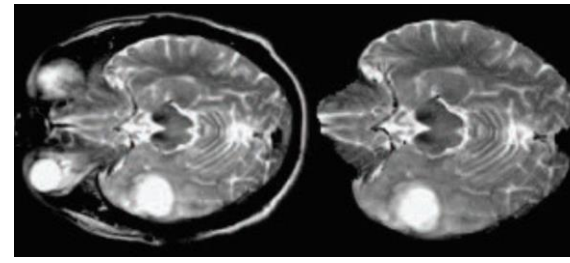

Fig. 3. The results of skull stripping from Bach Mai's dataset

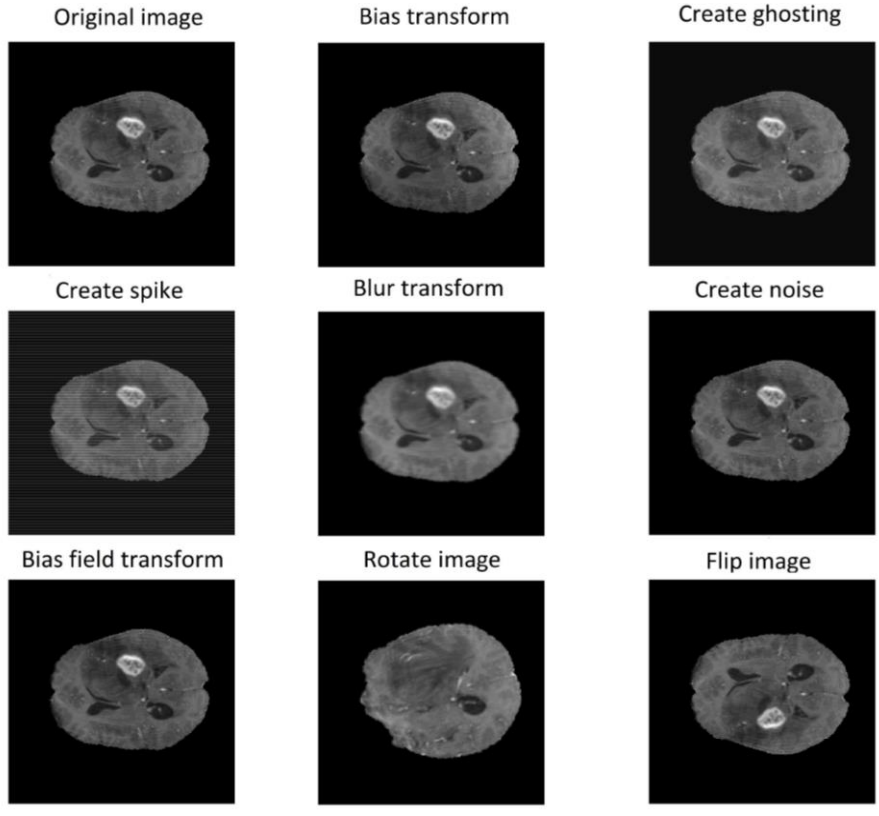

Fig. 4. Results of data augmentation of the training dataset

Figures 5, 6, and 7 depict the values of the loss function, the value of the DICE ratio, and the IoU value of the trained model with the newly processed dataset.

Figures 8 and 9 show the segmentation results of the trained model for test data (untrained data) in the BraTS2020 dataset and data collected from Bach Mai Hospital.

Table I compares the segmentation results of our model with some popular segmentation models.

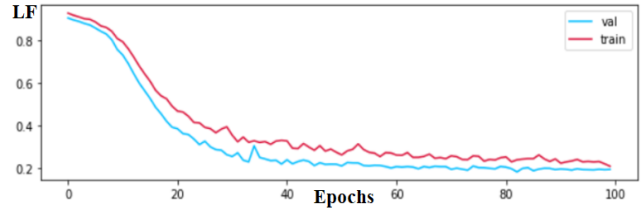

Fig. 5. Loss function (loss function) of the training process on the training (train) and validation (val) sets

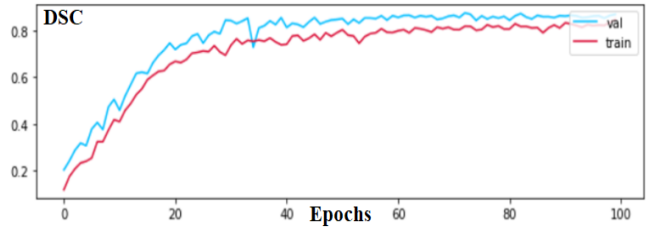

Fig. 6. Dice coefficient ratio of the trained model on the training (train) and validation (val) sets

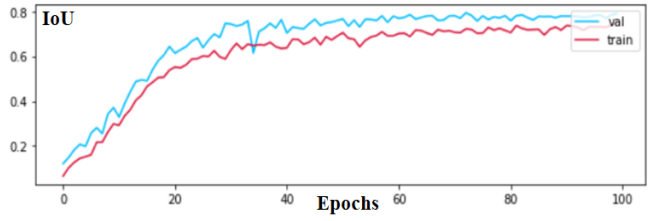

Fig. 7. The IoU value of the trained model on the training (train) and validation (val) sets

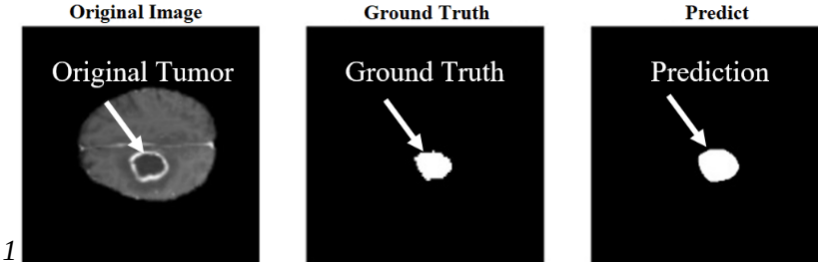

1

Fig. 8. The segmentation result of the tumor with the BraST2020 test dataset

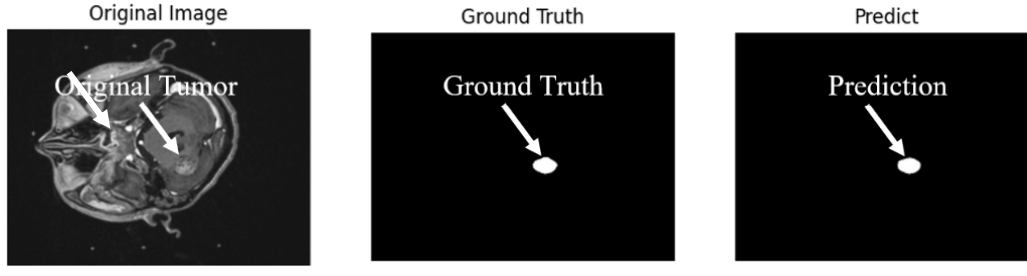

Fig. 9. The segmentation result of the tumor in Bach Mai's dataset

Table I. Comparison of brain tumor segmentation results for some models

Model	DICE Score	IoU
UNET [15]	0.870	0.795
ResU-Net [20]	0.873	0.792
AGResU-Net [22]	0.876	0.810
UNET++ (our)	**0.871**	**0.792**

B. Discuss

The results from Figure 3 show that the skull stripping tool we used can completely remove the skull cortex as well as the eye tissue while preserving the entire structure of the cerebral hemispheres. After the skull stripping process, the data collected from Bach Mai Hospital became similar to the data in the BraTS2020 dataset.

Figure 4 presents the outstanding results of eight processing techniques to augment the data and eliminate the effect of overfitting during training. In addition to the basic data augmentation techniques commonly used when training conventional segmentation models, data augmentation techniques such as bias transform, random ghosting, random spike, and random bias field were used to simulate the actual artifact during the acquisition and reconstruction of MRI. Through data augmentation, the efficiency of the training process can be improved, and the model is made better to be able to segment the actual magnetic resonance images.

From the training results shown in Figures 7, 8, and 9, it can be seen that that the loss function value of the model decreases quickly in the first 40 epochs, then the rate of change slows down. From epoch 80 to epoch 100, the value of the loss function decreases slowly. In the epoch range from 80 to 100, the DICE and IoU ratio values still increase, but their values do not change significantly. Thus, from 80 to 100 epochs can be used to train the model optimally. If the number of epochs, continues increasing, the training time will become very long while the model does not learn much. The trained model has the highest DICE ratio and the highest IoU value of 0.87 and 0.79, respectively. Thus, it is clear that the model can identify and segment tumors well from T1 magnetic resonance images.

Figure 9 shows the resulting segmentation image of the patient's brain tumor from the T1 MRI scheduled for radiosurgery at Bach Mai Hospital. The original tumor is the tumor segmented by the doctor, predicted tumor is the tumor segmented by our model. Basically, the tumor is segmented by the model having a similar location and shape to the tumor segmented by the radiologists; some healthy tissue in the brain is mistakenly segmented as a tumor. The total number of mislabeled and mistakenly segmented pixels is 20% less than the number of pixels in the ground truth, which is a poor number for the automatic segmentation model. However, if the model is used as a support tool, it can support the doctor quite well in the radiosurgery planning process. By using the model to preliminary segment brain tumors, radiologists only need to adjust the segmented tumor from the trained model instead of manually segmenting as before. Radiotherapy planning time will be shortened when the doctor uses the tumor segmentation model. Therefore, the doctor can focus on other work to improve the quality of the radiosurgery process.

Table I shows the predicted tumor of our model on the BraTS2020 dataset combined with the Bach Mai dataset

compared with other models using only the BraTS dataset. The segmentation model in this research that is trained with T1 images has a slightly lower segmentation precision than other trained models using all three types of MRIs (T1, T2, and FLAIR). The difference in segmental precision between our model and other models is trivial; it can be said that our model works well with a dataset consisting of only T1 images.

IV. CONCLUSION

In this research, we have successfully built a brain tumor segmentation model from T1 magnetic resonance imaging. The Focal Tversky Loss function was chosen to evaluate the training quality of the model because it gives the best performance in identifying the lesions. We built a program to remove the skull in the MRI images from Bach Mai to fuse the Bach Mai hospital and BraTS2020 datasets. The actual image segmentation results show that our model can accurately segment brain tumors. The model can be used to assist radiologists in the diagnostic process as well as in brain radiosurgery planning.

The training results of our model are slightly lower than those of models constructed by other research teams. The cause of this problem is that our model only uses T1 images for the training process, while the training datasets of other models include both T1 and T2 images as well as FLAIR images. In the future, we will customize and expand the model's structure and collect more data for the training dataset to further improve our model's performance. As a premise of this research, we hope that, with future improvements, it will make the brain tumor segmentation model and, more broadly, imaging diagnostics based on the deep learning approach, practical in clinical application.

ACKNOWLEDGMENTS

The work presented in this paper has been funded by the Vietnamese Ministry of Science and Technology, grant number ĐTCB.13/22/VKHKTHN. We also thank you for the Nuclear Medicine and Oncology Center at Bach Mai Hospital.

REFERENCES

[1]. Jerrold T. Bushberg Ph.D., J. Anthony Seibert Ph.D., Edwin M. Leidholdt Jr. Ph.D., John M. Boone Ph.D., "*The essential physics of medical imaging*," Lippincott Williams & Wilkins, pp. 8-9, 2002.

[2]. Rebecca, S., Diana, M., Eric, J., Choonsik, L., Heather, F., Michael, F., Robert, G., Randell, K., Mark, H., Douglas, M., et al. *"Use of Diagnostic Imaging Studies and Associated Radiation Exposure for Patients Enrolled in Large Integrated Health Care Systems,"* 1996–2010. JAMA 2012, 307, 2400 –2409.

[3]. Hsiao, C.-J., Hing, E., Ashman, J., *"Trends in electronic health record system use among office-based physicians: United States"*, 2007–2012. *Natl. Health Stat. Rep., 1*, pp. 1–18, 2014

[4]. Vincent S. Khoo, David P. Dearnaley, David J. Finnigan, Anwar Padhani, Steven F. Tanner, martin o. leach, "*Magnetic resonance imaging (MRI): considerations and applications in radiotherapy treatment planning*", Radiother Oncol, vol. 42, pp. 1-15, 1997.

[5]. Y, B. J. Matuszewski, Lik-Kwan Shark, C.J. Moore, "*A novel medical image segmentation method using dynamic programming*", IEEE, 2007, pp. 69-74.

[6]. H. Suzuki and J. Toriwaki, "Automatic segmentation of head MRI images by knowledge guided thresholding," *Computerized Med. Imag. Graphics*, vol. 15, no. 4, pp. 233–240, July–Aug. 1991.

[7]. C. Li, D. B. Godlgof, and L. O. Hall, "Knowledge-based classification and tissue labeling of MR images of human brain," *IEEE Trans. Med. Imag.*, vol. 12, pp. 740–750, Dec. 1993.

[8]. J. W. Snell, M. B. Merickel, J. M. Ortega, J. C. Goble, J. R. Brookeman, and N. F. Kassell, "Segmentation of the brain from 3-D MRI using a hierarchical active surface template," in *Proc. SPIE Conf. Medical Imaging*, 1994.

[9]. T. Kapur, W. E. L. Grimson, W. M. Wells III, and R. Kikinis, "Segmentation of brain tissue from magnetic resonance images," *Med. Imag. Anal.*, vol. 1, no. 2, 1996.

[10]. F. Pannizzo, M. J. B. Stallmeyer, J. Friedman, R. J. Jennis, J. Zabriskie, C. Pland, R. Zimmerman, J. P. Whalen, and P. T. Cahill, "Quantitative MRI studies for assessment of multiple sclerosis," *Magn. Reson. Med.*, vol. 24, pp. 90–99, 1992.

[11]. F. Gorunescu, "*Data mining techniques in computer-aided diagnosis: Non-invasive cancer detection*", PWASET 25, 427–430, 2007.

[12]. S. Minaee, Y. Y. Boykov, F. Porikli, A. J. Plaza, N. Kehtarnavaz and D. Terzopoulos, "*Image Segmentation Using Deep Learning: A Survey*" in *IEEE Transactions on Pattern Analysis and Machine Intelligence*, DOI: 10.1109/TPAMI.2021.3059968.

[13]. Suzuki, K. Overview of deep learning in medical imaging. *Radiol Phys Technol* **10,** 257–273 (2017). https://doi.org/10.1007/s12194-017-0406-5.

[14]. J. Long, E. Shelhamer and T. Darrell, "*Fully Convolutional Networks for Semantic Segmentation*," The IEEE Conference on Computer Vision and Pattern Recognition, pp. 3431-3440, 2015.

[15]. Olaf Ronneberger, Philipp Fischer, Thomas Brox, "U-Net: Convolutional Networks for Biomedical Image Segmentation", ArXiv: 1505.04597, 2015.

[16]. Z.W. Zhou, M.M.R. Siddiquee, N. Tajbakhsh, and J.M. Liang, "UNet++: A Nested U-Net Architecture for Medical Image Segmentation," Deep Learning in Medical Image Analysis and Multimodal Learning for Clinical Decision Support, pp: 3-11, 2018.

[17]. B. H. Menze, A. Jakab, S. Bauer, J. Kalpathy-Cramer, K. Farahani, J. Kirby, et al. "The Multimodal Brain Tumor Image Segmentation Benchmark (BRATS)", IEEE Transactions on Medical Imaging 34(10), 1993-2024 (2015) DOI: 10.1109/TMI.2014.2377694.

[18]. S. Bakas, H. Akbari, A. Sotiras, M. Bilello, M. Rozycki, J.S. Kirby, et al., "Advancing The Cancer Genome Atlas glioma MRI collections with expert segmentation labels and radiomic features", Nature Scientific Data, 4:170117 (2017) DOI: 10.1038/sdata.2017.117.

[19]. S. Bakas, M. Reyes, A. Jakab, S. Bauer, M. Rempfler, A. Crimi, et al., "Identifying the Best Machine Learning Algorithms for Brain Tumor Segmentation, Progression Assessment, and Overall Survival Prediction in the BRATS Challenge", arXiv preprint arXiv:1811.02629 (2018).

[20]. Foivos Diakogiannis, Francois Waldner, Peter Caccetta and Chen Wu, *"ResUNet-a: A deep learning framework for semantic segmentation of remotely sensed data"*, ISPRS Journal Photogrammetry and Remote Sensing, Vol 162, pp 94-114, 2020.

[21]. Jianxin Zhang, Zongkang Jiang, Jing Dong and Bin Liu, *"Attention Gate ResU-Net for Automatic MRI Brain Tumor Segmentation"*, *EEE Access*, vol. 8, pp. 58533-58545, 2020.